

# Diagrammatic representations of 3-periodic entanglements

TOKY ANDRIAMANALINA

MYFANWY E. EVANS

SONIA MAHMOUDI

Diagrams enable the use of various algebraic and geometric tools in analysing and classifying knots. In this paper we introduce a new diagrammatic representation of triply periodic entangled structures, which are embeddings of simple curves in  $\mathbb{R}^3$  that are invariant under translations along three non-coplanar axes. These diagrams require an extended set of new moves in addition to the Reidemeister moves, which we show to preserve ambient isotopies of triply periodic entangled structures. We use the diagrams to define the crossing number and the unknotting number of the triply periodic entanglements, demonstrating the practicality of the diagrammatic representation.

[57K10](#), [57K12](#); [57K35](#)

## 1 Introduction

A knot diagram is a planar projection of a knot, that is an embedding of  $\mathbb{S}^1$  in  $\mathbb{R}^3$ , with crossing information. It is a simple 2-dimensional representation that is very efficient in helping to understand the complexity of a 3-dimensional knot (see for example Adams [1]). A diagram allows one to translate the equivalence of knots given by ambient isotopies of the surrounding space  $\mathbb{R}^3$ , to simple moves on a plane called the *Reidemeister moves* (Figure 10) (see Burde, Zieschang and Heusener [4], Murasugi [33], Ozsváth, Stipsicz, and Szabó [36]). Knot diagrams enable the description of some numerical knot invariants, such as the crossing number or the unknotting number [1], and some algebraic knot invariants such as the Jones or Alexander polynomials (Lickorish [27]), among others.

While knots or links are compact structures, one can also consider ‘periodic knottings or linkings’ (Fukuda, Kotani and Mahmoudi [14], Morton and Grishanov [31]), which in the case of doubly periodic structures, called *2-structures* by Grishanov, Meshkov and Omelchenko in [16] or *DP tangles* by Diamantis, Lambropoulou and Mahmoudi

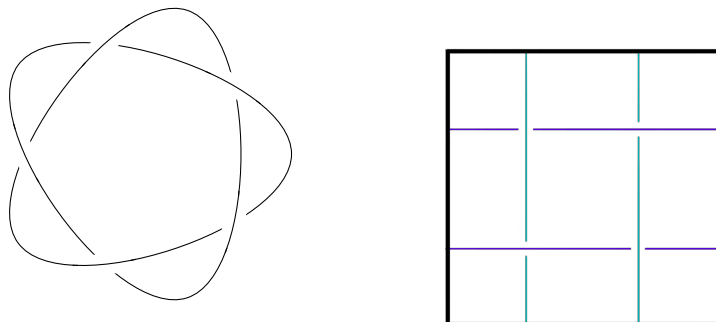


Figure 1: Diagrams of knotted structures: On the left, a diagram of the cinquefoil knot, drawn out of a planar projection of an embedding of the knot. On the right, a diagram of a doubly periodic alternating weave, drawn out of a projection of one of its unit cells onto a 2-torus, represented as a square with identified edges.

in [6], can be thought of as lifts in the universal cover of links in the thickened torus. As an infinite (doubly periodic) diagram of a DP tangle would contain infinitely many crossings, one may prefer to study diagrams of their unit cells, that are compact domains generating the whole DP tangle under translations, since they have less complexity. These diagrams are defined as link diagrams on a 2-torus  $\mathbb{T}^2$ , as illustrated in Figure 1 right (see Fukuda, Kotani and Mahmoudi [13], or Grishanov, Meshkov and Omelchenko [17, 18, 16]). As there are multiple choices of unit cells for a DP tangle, some complementary notions of equivalence have been added to account for these different unit cells as detailed in [6], such as *torus twists* [16] and *scale equivalence* [30], which respectively correspond to shearing the lattice or taking multiple copies of a unit cell.

There is interest in characterising entangled structures that are periodic in three directions of space (see for example Evans, Robins and Hyde [8], and also Hui and Purcell [24]), that we call *3-periodic tangles* or *TP tangles*. TP tangles are found in many different systems in the natural sciences. For example, the  $\Pi^+$  and  $\Sigma^+$  cylinder packings, which are packings of straight lines in  $\mathbb{R}^3$  (see O’Keeffe, Plévert, Teshima, Watanabe, and Ogama [34]) (Figure 2), are well known structures from structural chemistry which can be described as 3-periodic collections of curves embedded in  $\mathbb{R}^3$ . The  $\Sigma^+$  structure has been used to model the mesoscale structure of mammalian skin cells (corneocytes) (Evans and Hyde [7], Evans and Roth [9]), where the curves are helical rather than straight. Another setting where TP tangles are found is in DNA origami crystals (Seeman [39], Lu, Vecchioni, Ohayon, Sha, Woloszyn, Yang, Mao and Seeman [29]),

where the DNA strands tangle around each other to form a complicated 3-periodic structure. In polymeric systems, topological features of the entangled polymer chains influence their physical properties (Likhtman and Ponmurugan [28]), and thus some knot invariants have been extended into measures for periodic systems, such as the *periodic linking number* (Panagiotou [35]) or the *Jones polynomial* (Barkataki and Panagiotou [2]) to characterise the entanglement, where the invariants encompass both geometry and topology of the filaments.

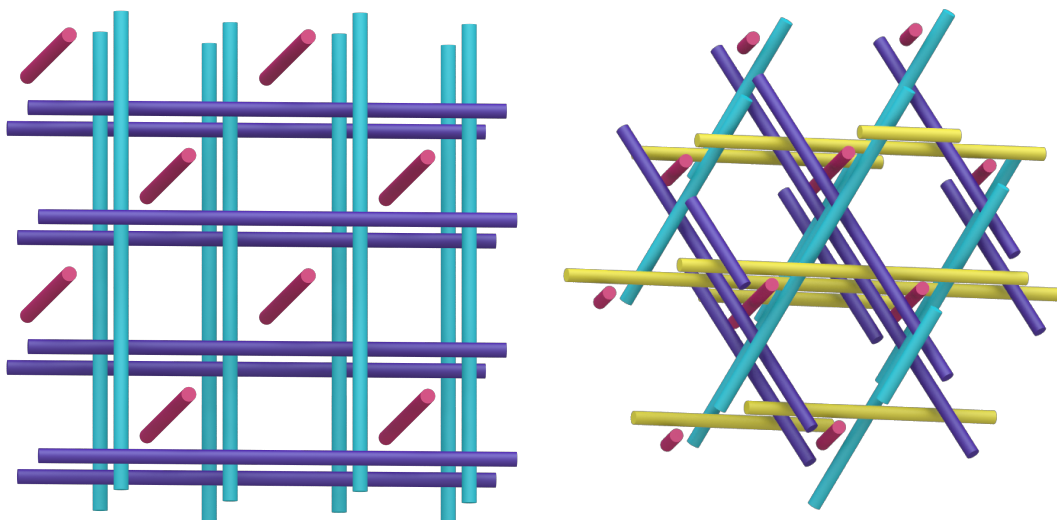


Figure 2: Simple examples of 3-periodic tangles are given by periodic packings of straight cylinders. These two structures are well known in structural chemistry, referred to as the  $\Pi^+$  cylinder packing on the left and the  $\Sigma^+$  cylinder packing on the right [34]. The cylinders are coloured by those that are parallel.

In this paper we describe a new diagrammatic representation of 3-periodic tangles, extending notions of equivalence to the 3-periodic setting. In Section 2 we present the definitions of 3-periodic tangles and the equivalence relation between them. Section 3 states the definitions of diagrams and *tridiagrams*, which are sets of three diagrams projected along three non-coplanar vectors, and their respective equivalences including two new moves added to the Reidemeister moves. We then state and prove a *generalised Reidemeister theorem* for 3-periodic tangles using singularity theory. Finally, in Section 4 we introduce some invariants such as the *crossing number* and the *unknotting number*.

## Acknowledgements

This work is funded by the Deutsche Forschungsgemeinschaft (DFG, German Research Foundation) - Project number 468308535, and partially supported by RIKEN iTHEMS.

## 2 3-periodic tangles and their equivalence

In this section, we give a definition of 3-periodic tangles. We then proceed by defining equivalence for such structures.

### 2.1 Definition of 3-periodic tangles

To define a 3-periodic tangle, we start by introducing different types of possible curve components.

**Definition 2.1** We call a *thread* an embedding of  $\mathbb{R}$  in  $\mathbb{R}^3$  having its two endpoints at infinity, and a *loop* an embedding of  $\mathbb{S}^1$  in  $\mathbb{R}^3$ .

**Remark 2.2** Note that curves that do not have both of their endpoints at infinity, like finite strands such as an embedding given by the arctangent map, are not included in the definition of a thread.

Thus, threads and loops form the components of the following object.

**Definition 2.3** An *entanglement* is a disjoint union, possibly infinite, of threads and loops in  $\mathbb{R}^3$ .

Therefore, we can define a 3-periodic tangle as a particular class of entanglement as follows.

**Definition 2.4** A *3-periodic tangle* or *TP tangle*  $K$  is an entanglement that is invariant under some 3-dimensional point lattice  $\Lambda$  which is isomorphic to  $\mathbb{Z}^3$ . When  $K$  is equipped with such a lattice, we denote the structure by  $\{K, \Lambda\}$ .

For 3-periodic tangles, we prefer working within a unit cell, that is a generating domain of a TP tangle, which has less complexity than the infinite structure.



**Definition 2.5** Let  $K$  be a 3-periodic tangle in  $\mathbb{R}^3$ . Let  $\{v_1, v_2, v_3\}$  be a basis of a lattice preserving the periodicity of  $K$ . By invariance under translation,  $K$  maps to the quotient space  $\mathbb{R}^3 / \mathbb{Z}.v_1 \oplus \mathbb{Z}.v_2 \oplus \mathbb{Z}.v_3 \cong \mathbb{T}^3$ . A *unit cell* of  $K$  is the quotient structure in the 3-torus  $\mathbb{T}^3 \cong \mathbb{S}^1 \times \mathbb{S}^1 \times \mathbb{S}^1$ , which can uniquely be described as a union of disjointly embedded closed curves in the 3-torus, ie a link embedded in  $\mathbb{T}^3$ .

**Remark 2.6** In a unit cell, a curve component homotopic to a point lifts into loops in the universal cover  $\mathbb{R}^3$ , and all the other curves lift into threads [10].

## 2.2 Equivalence of 3-periodic tangles

In general, one would like to tell whether two structures can continuously be deformed from one to the other. Clearly, there are affine transformations of  $\mathbb{R}^3$  that give rise to isotopic structures, such as rotations and translations of the TP tangle, or translations of the lattice associated to it. Shear deformations and uniform scalings of the TP tangle also give isotopic structures, where these correspond to deformations of the shape of a unit cell. All the following notions are true up to those transformations.

Although one can define equivalence classes of TP tangles using ambient isotopies in  $\mathbb{R}^3$ , we refine this definition to give a notion of equivalence that preserves the periodicity.

**Definition 2.7** Two 3-periodic tangles  $K$  and  $K'$  are said to be *p-equivalent* if there is an ambient isotopy  $H : \mathbb{R}^3 \times [0, 1] \longrightarrow \mathbb{R}^3 \times [0, 1]$  connecting them, for which there is a fixed lattice  $\Lambda$  under which  $K_t$  is invariant for all  $t \in [0, 1]$ , where  $K_0 = K$ , and  $K_1 = K'$  and  $K_t$  is the deformation of  $K$  to  $K'$  at  $t$ .

As the periodicity of a TP tangle is preserved by the *p*-equivalence, one can use a unit cell to understand the transformation. For a comprehensive diagrammatic description however, we prefer giving another definition of equivalence, starting directly from a unit cell and involving only the unit cell and not the full 3-periodic tangle. For a TP tangle, there are multiple choices of unit cells as shown in Figure 3. Any unit cells taken out of different lattices should be somehow related as they represent the same TP tangle.

From the same lattice, there are many possible unit cells that can be obtained. Consider a 3-periodic tangle  $K$  with a given lattice  $\Lambda$ . Assume that  $\Lambda$  is  $\mathbb{Z}^3$  and regard it as a  $\mathbb{Z}$ -module generated by vectors of  $\mathbb{R}^3$ , ie a set of linear combinations of vectors of  $\mathbb{R}^3$  with scalars in  $\mathbb{Z}$ . Two different sets of generators give rise to two different unit cells.

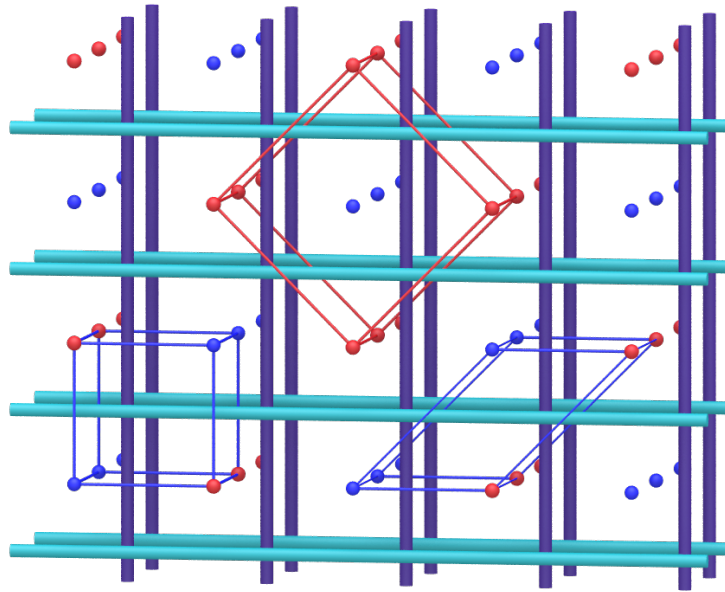


Figure 3: Two different lattices (represented by red points and blue points, the red ones belonging to the blue lattice as well) that preserve the periodicity of the TP tangle. Different unit cells can be taken out of those lattices, like the blue cube and the blue parallelepiped both belonging to the blue lattice or the red parallelepiped which is a unit cell of volume 2 with respect to the blue lattice.

A change of basis of  $\mathbb{Z}^3$ , which preserves the orientation, is given by a matrix  $M$  of  $SL(3, \mathbb{Z})$ . But such a matrix induces an orientation-preserving linear homeomorphism of  $\mathbb{R}^3$  that is equivariant with respect to the deck transformation group  $\mathbb{Z}^3$ , and thus descends to a linear homeomorphism  $\phi_M$  of the torus  $\mathbb{T}^3 = \mathbb{R}^3/\mathbb{Z}^3$  [11].

**Example 2.8** For illustration, consider  $M_1 = \begin{bmatrix} 1 & 0 & 0 \\ -1 & 1 & 0 \\ 0 & 0 & 1 \end{bmatrix}$ .

Consider the unit cell given in Figure 4a. The idea to visualise the action of  $\phi_{M_1}$  on this unit cell is to glue four faces of the cube delimiting  $\mathbb{T}^3$ , to get a thickened 2-torus with the inner and outer surfaces being identified as in Figure 4b. The map  $\phi_{M_1}$  acts on the thickened torus with identified surfaces by twisting it as shown in Figure 4c. By gluing four faces of the unit cell of Figure 4d, one gets the twisted torus of Figure 4c. Such a move is called a torus twist, and therefore, the two unit cells of Figures 4a and 4d are connected by a torus twist.

Independently of any matrix of  $\mathbb{R}^n$  where  $n$  is 2 or 3, a torus twist can be described at the level of the  $n$ -torus as follows.

Consider the compact manifold with boundary  $A = [0, 1] \times (\mathbb{S}^1)^{n-1}$ . To orient  $A$ , one can embed it in  $\mathbb{R}^m$  with  $m$  well chosen depending on  $n$ , and take the orientation induced by that of  $\mathbb{R}^m$ . See Figure 5a left for the case  $n = 2$ .

Let  $T : A \rightarrow A$  be the map defined by

$$T(t, \theta, \psi) = (t, \theta + 2\pi t, \psi).$$

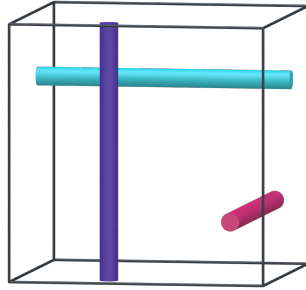
$T$  is an orientation preserving map that fixes  $\partial A = \{0, 1\} \times (\mathbb{S}^1)^{n-1}$  pointwise, as shown in Figure 5a. Notice that we can choose  $\theta + 2\pi kt$  with any integer  $k$  to get any type of twist.

Now consider  $\alpha$  a closed curve embedded in  $\mathbb{T}^n$ . Let  $N$  be a regular neighbourhood of  $\alpha$  and choose an orientation-preserving homeomorphism  $g : A \rightarrow N$ . The map

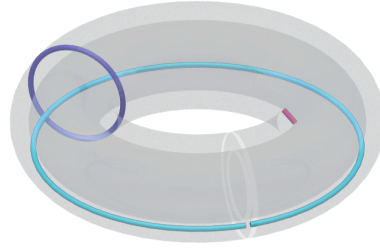
$$T_g(x) = \begin{cases} g \circ T \circ g^{-1}(x) & x \in N \\ x & x \in \mathbb{T}^n \setminus N \end{cases}$$

is a torus twist, as seen in Figure 5b [12].

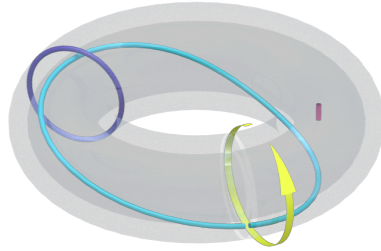
In the case of TP tangles, as all  $\phi_M$ 's with  $M$  transvection matrices, can be described by 3-torus twists, all other  $\phi_M$ 's with any  $M$  in  $SL(3, \mathbb{Z})$  can be described by finite combinations of 3-torus twists. Thus, any two unit cells of the same lattice are connected



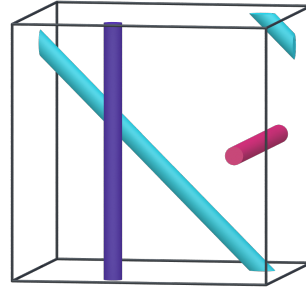
(a) Unit cell of a simple packing of cylinders.



(b) Same unit cell as that of (A) represented as a thickened 2-torus with identified inner and outer surfaces.



(c) Action of  $\phi_{M_1}$  on the thickened 2-torus with identified surfaces.



(d) Resulting unit cell after the action of  $\phi_{M_1}$ .

Figure 4: Visualisation of the action of  $\phi_{M_1}$  on a unit cell of a simple TP tangle.

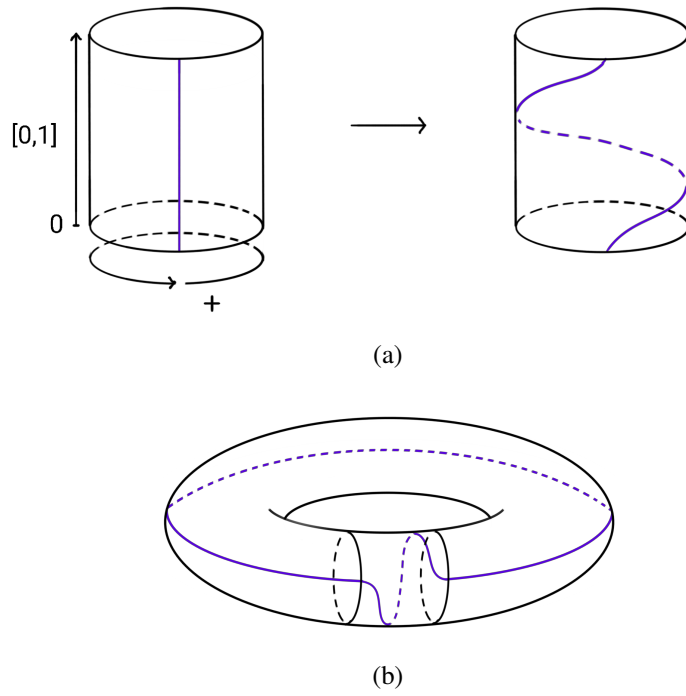


Figure 5: A torus twist of a 2-torus: On the top, a twist of the annulus  $A = [0, 1] \times \mathbb{S}^1$ . On the bottom, the resulting torus after embedding the twisted annulus.

by a finite sequence of 3-torus twists.

We now give a notion of equivalence of curves mapped in tori that are connected by torus twists. We generalise the definition to the cases  $n = 2$  or  $3$ .

**Definition 2.9** Two collections of closed curves mapped in  $\mathbb{T}^n$ ,  $\Gamma_1$  and  $\Gamma_2$ , are  $T^n$ -equivalent if they are connected by a finite sequence of  $n$ -torus twists.

**Remark 2.10** Strictly speaking, a torus twist  $T_g$  (independently of any matrix) has been defined only for embeddings of closed curves. However, in Definition 2.9 we extend the notion to any mappings of curves as it can be understood for all cases.

**Remark 2.11** Definition 2.9 generalises the notion of equivalence of motifs of DP tangles under Dehn twists for a fixed lattice, called *Dehn equivalence* in [6], first explained in [16]. In particular, the notion of  $n$ -torus twists is an extension of the notion of Dehn twists for tori in dimension 3 [12].

There can be many lattices preserving the periodicity of a TP tangle. Should there be two lattices  $\Lambda$  and  $\Lambda'$  preserving the periodicity of a TP tangle, if  $A = \{u_1, u_2, u_3\}$  and  $A' = \{u'_1, u'_2, u'_3\}$  are two respective bases, then the lattice  $\Lambda_0$  generated by  $A \cup A'$  also preserves the periodicity of the TP tangle. Thus, whenever one finds two such lattices, they are subgroups of a group which also preserves the periodicity of the TP tangle.

**Definition 2.12** For a 3-periodic tangle  $K$  with a given lattice  $\Lambda_1$ , a lattice  $\Lambda_2$  is called a *refinement* of  $\Lambda_1$  if  $\Lambda_1$  is a subgroup of  $\Lambda_2$  and if  $\Lambda_2$  also leaves  $K$  invariant.

Suppose, for a TP tangle  $K$ , we have  $\Lambda_2$  a refinement of  $\Lambda_1$ . Without loss of generality, assume that  $\Lambda_2$  is  $\mathbb{Z}^3$  endowed with its usual basis. Since  $\Lambda_1$  is a point lattice and is a subgroup of  $\Lambda_2$ , it is of type  $\mathbb{Z}.k_1e_1 \oplus \mathbb{Z}.k_2e_2 \oplus \mathbb{Z}.k_3e_3$  where the  $k_i$ 's are positive integers and the  $e_i$ 's the canonical vectors of space. As  $\mathbb{Z}^3$  is the fundamental group of  $\mathbb{R}^3$  and as this latter is simply connected, by the connection between subgroups of the fundamental group and path-connected covering spaces of  $\mathbb{R}^3/\mathbb{Z}^3$ , called Galois connection [21], there is a cover

$$\mathbb{R}^3/\Lambda_1 \longrightarrow \mathbb{R}^3/\mathbb{Z}^3.$$

Pictorially,  $\mathbb{R}^3/\Lambda_1$  is a multiple of  $\mathbb{R}^3/\mathbb{Z}^3$  as given in Example 2.13.

**Example 2.13** Suppose  $\Lambda_1 = \mathbb{Z}.2e_1 \oplus \mathbb{Z}.e_2 \oplus \mathbb{Z}.e_3$ . Consider the TP tangle having a unit cell displayed in Figure 4a. In this case, the cover map is

$$\begin{aligned} \mathbb{R}^3 / \mathbb{Z}.2e_1 \oplus \mathbb{Z}.e_2 \oplus \mathbb{Z}.e_3 &\cong \mathbb{S}^1 \times \mathbb{S}^1 \times \mathbb{S}^1 \longrightarrow \mathbb{S}^1 \times \mathbb{S}^1 \times \mathbb{S}^1 \cong \mathbb{R}^3 / \mathbb{Z}^3 \\ (z_1, z_2, z_3) &\longmapsto (z_1^2, z_2, z_3), \quad z_i \in \mathbb{C}, \end{aligned}$$

and the unit cell corresponding to the lattice  $\mathbb{Z}.2e_1 \oplus \mathbb{Z}.e_2 \oplus \mathbb{Z}.e_3$  is the double of the one of Figure 4a along the  $x$ -axis as seen in Figure 6.

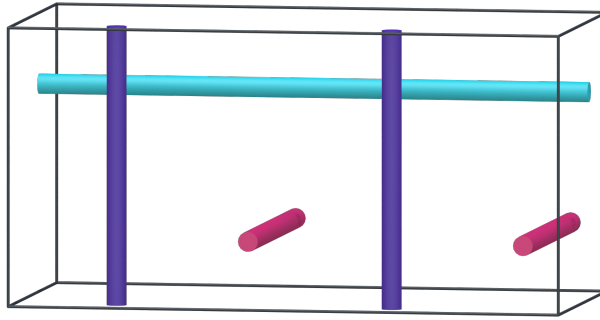


Figure 6: A unit cell of the simple packing of cylinders of Figure 4 corresponding to the lattice  $\mathbb{Z}.2e_1 \oplus \mathbb{Z}.e_2 \oplus \mathbb{Z}.e_3$ , that is of volume twice that of the unit cell in Figure 4a.

In the following, we state a notion of equivalence for curves mapped in tori that are connected by cover maps. The definition is given for the cases  $n = 2$  or  $3$ .

**Definition 2.14** Two collections of closed curves in  $n$ -tori,  $\Gamma$  and  $\Gamma'$ , are  $M^n$ -equivalent if there is a sequence of collections of closed curves in  $n$ -tori  $(\Gamma_k)_{k=0, \dots, m}$  where  $\Gamma_0 = \Gamma$ ,  $\Gamma_m = \Gamma'$ , and for all  $k = 1, \dots, m$ , either  $\Gamma_{k-1}$  is a cover  $\Gamma_k$  or  $\Gamma_k$  is a cover  $\Gamma_{k-1}$ , where the cover map is of type

$$\begin{aligned} \underbrace{\mathbb{S}^1 \times \dots \times \mathbb{S}^1}_n &\longrightarrow \underbrace{\mathbb{S}^1 \times \dots \times \mathbb{S}^1}_n \\ (z_1, \dots, z_n) &\longmapsto (z_1^{k_1}, \dots, z_n^{k_n}), \quad z_i \in \mathbb{C}, k_i \in \mathbb{Z}_{>0}. \end{aligned}$$

In general not all 3-periodic tangles are worth our attention. One example that one wants to avoid is a periodic embedding of the wild knot invented by R.H. Fox [4]. Another example is an embedding of parallel lines along the  $z$ -axis passing through every point  $(p, q, 0) \in \mathbb{Q}.(1, 0, 0) \oplus \mathbb{Q}.(0, 1, 0)$ . The structure is 3-periodic, but within any of its unit cells there are infinitely many components. This motivates the definition of *tame* 3-periodic tangles.

**Definition 2.15** A 3-periodic tangle is called *tame* if one of its unit cells is ambient isotopic to a disjoint union of finitely many simple closed polygons in  $\mathbb{T}^3$  (polygonal links in  $\mathbb{T}^3$ ). A structure is called *wild* if it is not tame.

**Remark 2.16** Definition 2.15 is true regardless of the unit cell chosen due to the previous remarks we made on relations between unit cells via  $T^3$ -equivalence and  $M^3$ -equivalence.

An immediate consequence is that the *most refined lattice* of a tame TP tangle exists, which is not true for the second example we had given for wild structures. We denote the most refined lattice by  $\mathcal{L}^*$ , which generalises the notion of *minimal lattice* for DP tangles [6].

From now on, we only consider tame 3-periodic tangles, and we define their equivalence as follows.

**Definition 2.17 (Equivalence of 3-periodic tangles)**

Let  $\{K, \Lambda\}$  and  $\{K', \Lambda'\}$  be two 3-periodic tangles with given point lattices  $\Lambda$  and  $\Lambda'$ . They are *equivalent* if there is a sequence of links in  $\mathbb{T}^3$ ,  $(\Gamma_k)_{k=0, \dots, n}$  for which we have,  $\Gamma_0$  a unit cell of  $\{K, \Lambda\}$ ,  $\Gamma_n$  a unit cell of  $\{K', \Lambda'\}$  and for all  $k = 1, \dots, n$ ,  $\Gamma_{k-1}$  and  $\Gamma_k$  are either ambient isotopic, or  $T^3$ -equivalent as given by Definition 2.9 or  $M^3$ -equivalent as given by Definition 2.14.

**Proposition 2.18** Two TP tangles  $K$  and  $K'$  are  $p$ -equivalent if and only if they are equivalent in the sense of Definition 2.17.

**Proof** If  $K$  and  $K'$  are  $p$ -equivalent, by descending into the quotient space, one obtains isotopic unit cells. Conversely, subdivide the interval  $[0, 1]$  into smaller intervals  $[t_{k-1}, t_k]$ , where  $k$  ranges over the indices  $\{0, \dots, n\}$  of the sequence given in Definition 2.17. By lifting the  $\Gamma_k$ 's to  $\mathbb{R}^3$ , one notices that ambient isotopies of  $\mathbb{T}^3$  lift into ambient isotopies of  $\mathbb{R}^3$ , and torus twists and  $M^3$ -equivalence lift into the identity map of  $\mathbb{R}^3$  as they only represent choices of unit cells. This gives an isotopy connecting  $K$  and  $K'$  and a lattice  $\bigcap_{k=0, \dots, n} \Lambda_k$  satisfying the conditions of Definition 2.7, where  $\Lambda_k$  is the lattice naturally associated to the lift of  $\Gamma_k$ .  $\square$

### 3 Reidemeister theorem for diagrams of 3-periodic tangles

In this section, we formalise the diagrammatic description of 3-periodic tangles, and define the notions of equivalence for diagrams. Then, we prove a generalised Reidemeister theorem for 3-periodic tangles.



### 3.1 Diagrams

Our aim is to encode the 3-dimensional topological information of TP tangles into 2-dimensional diagrams. In classical knot theory, one can obtain a diagram by projecting a knot onto a plane and by adding crossing information to the projection. In the following, we generalise this approach by making a projection of a unit cell of a TP tangle onto a 2-torus represented as a square with identified edges.

Note that projecting the 3-torus  $\mathbb{T}^3 \cong \mathbb{S}_1^1 \times \mathbb{S}_2^1 \times \mathbb{S}_3^1$  represented as a cube with identified faces onto a 2-torus, say  $\mathbb{T}_1^2 \cong \mathbb{S}_1^1 \times \mathbb{S}_2^1$ , can be seen as flattening  $\mathbb{S}_3^1$ . It is important to keep track of the two identified faces along  $\mathbb{S}_3^1$  as they are indistinct on the 2-torus. Just as with crossings for usual knots with an over-strand and an under-strand, a point intersecting those faces must also carry the information of which part is over and which is under. To capture this, we start with parametrising  $\mathbb{S}_3^1$  as follows.

We recall that  $\mathbb{S}^1$  is smoothly diffeomorphic to a union of an open interval and a point  $(0, 1) \cup \{N\}$ . One possibility to get this is by considering an atlas given by two stereographic projections from the North and South poles, each of which transforms the punctured circle into the real line  $\mathbb{R}$  [26]. By composing one stereographic map with the smooth map  $s : x \mapsto \frac{1}{\pi} \arctan(x) + \frac{1}{2}$ , one gets the open interval  $(0, 1)$ . This gives rise to two smooth maps  $f_N : \mathbb{S}^1 \times \mathbb{S}^1 \times (\mathbb{S}^1 \setminus \{N\}) \rightarrow \mathbb{S}^1 \times \mathbb{S}^1 \times (0, 1)_N$  and  $f_S : \mathbb{S}^1 \times \mathbb{S}^1 \times (\mathbb{S}^1 \setminus \{S\}) \rightarrow \mathbb{S}^1 \times \mathbb{S}^1 \times (0, 1)_S$  and a smooth map transitioning between them. Those three maps fully describe the 3-torus.

We represent  $\mathbb{S}_1^1 \times \mathbb{S}_2^1 \times (0, 1)_N$  as a cube with identified opposite faces, save the front and back ones, where we define the front and back faces of a 3-torus and of  $\mathbb{S}_1^1 \times \mathbb{S}_2^1 \times (0, 1)_N$  as follows.

**Definition 3.1** Consider the 3-torus  $\mathbb{T}^3 \cong \mathbb{S}_1^1 \times \mathbb{S}_2^1 \times \mathbb{S}_3^1$ . The *front face* of the torus is defined as  $\mathbb{S}_1^1 \times \mathbb{S}_2^1 \times \{0 + \varepsilon\}$  of  $\mathbb{S}_1^1 \times \mathbb{S}_2^1 \times (0, 1)_N$ , and the *back face* is defined as  $\mathbb{S}_1^1 \times \mathbb{S}_2^1 \times \{1 - \varepsilon\}$ , with  $\varepsilon > 0$  arbitrarily small. The submanifold  $\mathbb{S}_1^1 \times \mathbb{S}_2^1 \times \{N\}$  of  $\mathbb{S}_1^1 \times \mathbb{S}_2^1 \times (0, 1)_S$  is referred to as the *N-face*.

Let  $l$  be a link in  $\mathbb{T}^3$ . It follows that the embedding of  $l$  in  $\mathbb{T}^3$  has two descriptions via the two maps  $f_N$  and  $f_S$ . Note that as those two maps and the map transitioning between them are all smooth, they preserve the smoothness of the curves when  $l$  is smoothly embedded.

Consider the projection map  $\pi : \mathbb{T}^3 \longrightarrow \mathbb{T}_1^2$  which is described by the maps  $\pi_N : \mathbb{S}_1^1 \times \mathbb{S}_2^1 \times (0, 1)_N \longrightarrow \mathbb{T}_1^2$  via  $f_N$  and  $\pi_S : \mathbb{S}_1^1 \times \mathbb{S}_2^1 \times (0, 1)_S \longrightarrow \mathbb{T}_1^2$  via  $f_S$ . Visually, we consider the information given by  $\pi_N$  as in Figure 7. The map  $\pi_S$  is used only to complete the missing pieces of information on the  $N$ -face. By doing so, one can understand the ‘height’ of a curve, especially regarding the front face and back face from Definition 3.1. If one considers  $\mathbb{S}_1^1 \times \mathbb{S}_2^1 \times (0, 1)_N \longrightarrow (0, 1)$ , one can regard it as a map that determines the ‘height’ of  $\mathbb{S}_1^1 \times \mathbb{S}_2^1 \times \{t\}$  on  $(0, 1)$ . Visualising the map  $\mathbb{S}_1^1 \times \mathbb{S}_2^1 \times \mathbb{S}_3^1 \longrightarrow \mathbb{S}_3^1$  as a ‘height map’ is difficult as  $\mathbb{S}_3^1$  loops around. Given this, we can introduce new symbols to represent a point intersecting the  $N$ -face.

**Notation 3.2** The thick dot in Figure 8 left called *F-point* depicts an ‘intersection with the front face’, and the circle in Figure 8 right called *B-point* depicts an ‘intersection with the back face’.

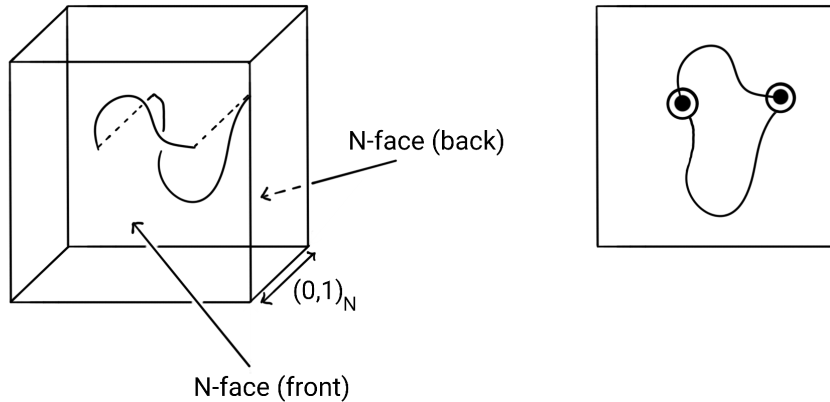


Figure 7: Drawing out a diagram of a 3-periodic tangle: on the left, a link with a single component in the 3-torus. One circle of the torus is represented as the union of the open interval  $(0,1)$  and the North point  $N$ . The identified front and back faces are called the  $N$ -face. On the right, the resulting diagram with a symbol representing the points belonging to the  $N$ -face.

Note that a point  $P \in \pi(l)$  with  $\pi^{-1}(P)$  containing more than one point of  $l$  is called a *multiple point*.

Diagrams of knotted structures are drawn in *regular projections*, avoiding ambiguity in aspects like the nature of a crossing of a triple point [4]. For similar reasons, we want to define a notion of regular projection for TP tangles. To do so, we can restrict our curves



Figure 8: New symbols: on the left, the  $F$ -point, representing the part of the curve that is close to the front face  $\mathbb{S}_1^1 \times \mathbb{S}_2^1 \times \{0 + \varepsilon\}$ . On the right, the  $B$ -point, representing the part of the curve that is close to the back face  $\mathbb{S}_1^1 \times \mathbb{S}_2^1 \times \{1 - \varepsilon\}$ .

to smoothly embedded ones as the set of such curves is dense in the set of embeddings of curves [22]. We make use of the genericness of transversality, meaning that the set of transverse maps with respect to a manifold is dense in the set of smooth maps. This is a consequence of Thom's transversality theorem which states the following. Suppose  $f_t : X \rightarrow Y$  is a family of smooth maps indexed by a parameter  $t$  that ranges over some set  $T$ . Consider the map  $F : X \times T \rightarrow Y$  defined by  $F(x, t) = f_t(x)$ . We require that the family varies smoothly by assuming  $T$  to be a manifold and  $F$  to be smooth.

**Theorem 3.3** (Thom, [40]). *Suppose that  $F : X \times T \rightarrow Y$  is a smooth map of manifolds, where only  $X$  has boundary, and let  $Z$  be any boundaryless submanifold of  $Y$ . If both  $F$  and  $\partial F$  are transversal to  $Z$ , then for almost every  $t \in T$ , both  $f_t$  and  $\partial f_t$  are transversal to  $Z$ .*

A proof of Theorem 3.3 can be found in [20, 23].

As an example, in our case the transversality theorem implies that any curve in  $\mathbb{T}^2$  may be deformed by an arbitrarily small amount to have a transverse intersection with a second curve as in Figure 9.

This allows us to state the following definition.

**Definition 3.4 (Regular projection)**

We say that a projection  $\pi$  of a link  $l$  in  $\mathbb{T}^3$  is called *regular*, or that  $l$  is in *general position* with respect to the projection  $\pi$ , if  $\pi$  satisfies the following five requirements:

- (1) there are only finitely many multiple points  $\{P_i : 1 \leq i \leq n\}$ , and all multiple points are double points, that is  $\#\pi^{-1}(P_i) = 2$ .
- (2) all intersections, ie double points, are transverse.
- (3) no point in the  $N$ -face is mapped onto a double point.

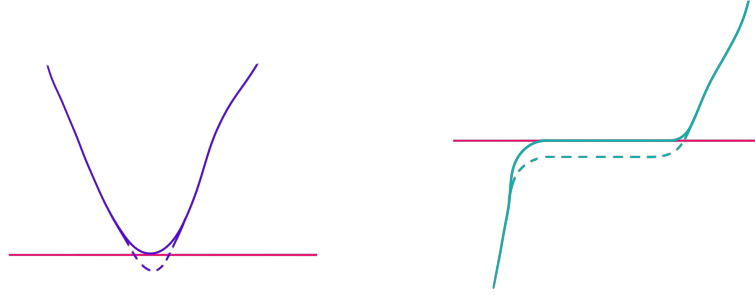


Figure 9: Deforming curves to get transverse intersections.

- (4) in  $\mathbb{T}^3$ , all intersections of a link component with the  $N$ -face are transverse.
- (5) consider the borders of the square torus as its generating circles  $l_1$  and  $l_2$ , and regard those circles as embedded curves in the torus. Each point of the projected curves of the link intersecting  $l_1$  and  $l_2$  is not a double point, and does not belong to the  $N$ -face. Moreover, all intersections with  $l_1$  and  $l_2$  are transverse.

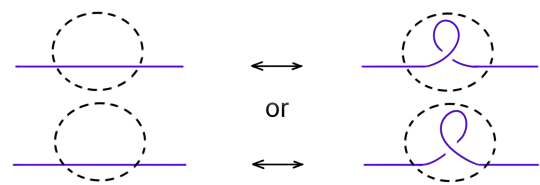
**Definition 3.5** A *diagram* of a TP tangle is a regular projection of one of its unit cells, with crossing information, together with  $F$ -points and  $B$ -points.

**Remark 3.6** Unlike in the case of DP tangles where we define the notion of an *infinite diagram* [13] representing the entire doubly periodic structure, we do not state a similar definition for TP tangles.

### 3.2 Notions of equivalence of diagrams

Ambient isotopies of usual knots in  $\mathbb{R}^3$  are translated at the diagrammatic level to planar isotopies and Reidemeister moves [4]. We recall that the first Reidemeister move ( $R_1$ ) allows us to put in or take out a twist in the knot, which also adds or removes a crossing as shown in Figure 10a. The second Reidemeister move ( $R_2$ ) adds or removes two crossings as displayed in Figure 10b. The third Reidemeister move ( $R_3$ ) allows us to slide a strand of the knot from one side of a crossing to the other side of the crossing, as depicted in Figure 10c.

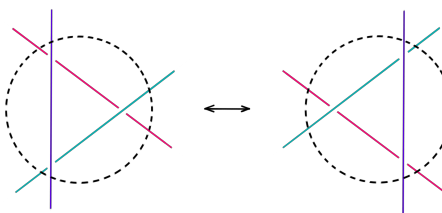
In the case of TP tangles, we introduced new diagrammatic symbols (Figure 8) to describe the direction of periodicity along which the projection is made. New moves arise due to these new symbols.



(a) The  $R_1$  move



(b) The  $R_2$  move



(c) The  $R_3$  move

Figure 10: The three Reidemeister moves.

**Definition 3.7** The  $R_4$  move depicts a strand of the link which slides between the front part and back part of another strand that goes through the  $N$ -face as in shown Figure 11a. The  $R_5$  move allows us to pass a part of a curve through the  $N$ -face as seen in Figure 11b. We call  $R$ -moves the set of five moves given by the three Reidemeister moves and the  $R_4$  and  $R_5$  moves.

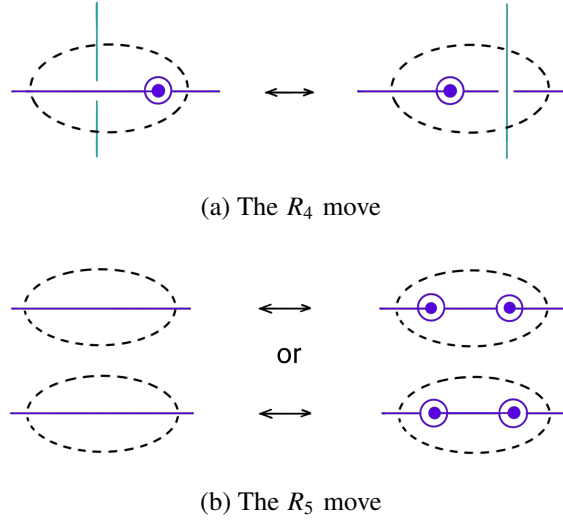


Figure 11: The two new moves, necessary for 3-periodic tangles.

For illustration, note that the  $R_4$  and  $R_5$  moves respectively mimic the isotopies that transform the unit cell of Figure 12a to that of Figure 12b (or vice-versa) and the unit cell of Figure 12c to that of Figure 12d (or vice-versa).

**Remark 3.8** In Figure 10a on the  $R_1$  move, the second alternative can be obtained by a finite sequence of the first alternative and  $R_2$  and  $R_3$  moves [33]. We list the two variants only because both are needed for the proof of the generalised Reidemeister theorem that will be given later in the paper, where an isotopy is locally translated to one variant of each  $R$ -move and not a sequence of variants. On the other hand, the two alternatives for an  $R_5$  move in Figure 11b are not connected by any sequence of other  $R$ -moves.

Aside from ambient isotopies of the 3-torus, the other notions needed for the equivalence of TP tangles, such as the torus twists or the  $M^3$ -equivalence for example, also need to

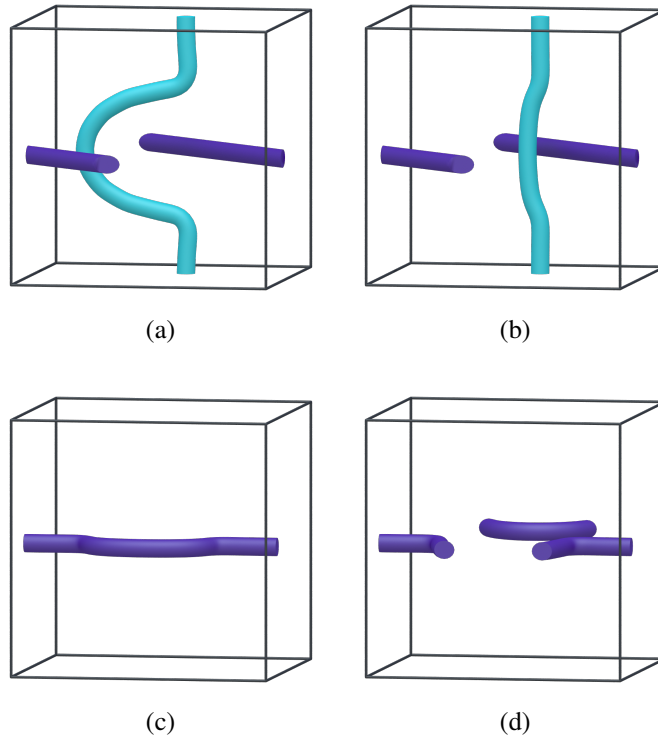


Figure 12: Ambient isotopies that cannot be realised with the usual Reidemeister moves in a diagram: On the top, an isotopy from (A) to (B) or vice-versa that would correspond to the  $R_4$  move in a diagram. On the bottom, an isotopy from (C) to (D) or vice-versa that would correspond to the  $R_5$  move in a diagram.

be described at the diagrammatic level.

Consider a unit cell of a TP tangle and suppose that one projects to a diagram as described above. It is clear that one can also get another diagram by projecting the cube from the back side, by inverting all the notions of front and back faces as well as  $F$  and  $B$ -points of Notation 3.2. As the diagrams from the front and back sides represent the same 3-periodic tangle, there should be an equivalence relation between them. We recall that the closure of the complement of a solid torus in the 3-sphere is again a solid torus [37]. Map a diagram  $D$  onto the surface of a solid torus in  $\mathbb{S}^3$ . The pattern on the surface of the solid torus is inverted on the surface of its complement, just like looking at a diagram from its back. The crossings are inverted and so are the  $F$ -points and  $B$  ones. This gives the desired equivalence relation.

We may now define all the necessary notions of equivalence for diagrams.

**Definition 3.9** Consider two diagrams  $D_1$  and  $D_2$ .

- (1) They are *R-equivalent* if they are connected by a finite sequence of  $R$ -moves and planar (2-torus) isotopies. We denote the equivalence by  $D_1 \sim_R D_2$ .
- (2) They are  *$T^2$ -equivalent* if they are connected by a finite sequence of 2-torus twists, as given in Definition 2.9. We denote the equivalence by  $D_1 \sim_{T^2} D_2$ .
- (3) They are  *$M^2$ -equivalent* if they satisfy the conditions of Definition 2.14, where they are related by different covering maps. We denote the equivalence by  $D_1 \sim_{M^2} D_2$ .
- (4) They are *V-equivalent* if  $D_1 = D_2$  or if  $D_2$  is obtained by considering  $D_1$  on its ‘complementary torus’ as described above. We denote the equivalence by  $D_1 \sim_V D_2$ .

We wrap up all these notions of equivalence into one in the following.

**Definition 3.10** Two diagrams  $A$  and  $B$  are called *D-equivalent*, or just *equivalent*, if there is a finite sequence of diagrams  $(D_k)_{k=0, \dots, n}$ , for which we have

$$D_0 = A, \quad D_n = B \quad \text{and} \quad \left\{ \begin{array}{ll} D_{k-1} \sim_R D_k \\ \text{or} \\ D_{k-1} \sim_{T^2} D_k \\ \text{or} \\ D_{k-1} \sim_{M^2} D_k \\ \text{or} \\ D_{k-1} \sim_V D_k \end{array} \right. \quad \forall k = 1, \dots, n.$$



We denote the equivalence by  $A \sim_D B$ .

**Remark 3.11** Unless otherwise mentioned, we always refer to this definition whenever we talk about equivalence of diagrams.

Before formulating our generalised Reidemeister theorem for 3-periodic tangles, we state an implication of the Reidemeister theorem for links in the 3-torus using the diagrams as defined in this paper. It is important to note that other generalisations of the Reidemeister theorem for (oriented) links in the 3-torus have been proven in the literature, such as in [25] where one makes use of mixed link diagrams.

**Theorem 3.12** *Two TP tangles  $K$  and  $K'$ , for which there are two unit cells  $\Gamma$  and  $\Gamma'$  connected by ambient isotopies, possess equivalent diagrams.*

To prove this theorem, we extend to TP tangles the already known proof for usual knots in  $\mathbb{R}^3$  using singularity theory [36, 38]. Without loss of generality, we can assume that the unit cells  $\Gamma$  and  $\Gamma'$  are links in  $\mathbb{T}^3$  with one component. The proof of the general case is similar.

We are going to prove that supposing the two 1-component links  $\Gamma$  and  $\Gamma'$  are ambient isotopic, the isotopy  $[0, 1] \times \mathbb{S}^1 \longrightarrow [0, 1] \times \mathbb{T}^3$  between them gives rise to a 1-parameter family of diagrams which are connected by planar isotopies and  $R$ -moves. Indeed, if one keeps track of the isotopy parameter  $t \in [0, 1]$ , one can project  $[0, 1] \times \mathbb{T}^3$  onto  $[0, 1] \times \mathbb{T}^2$  and compose the isotopy and the projection to obtain a map from the 2-manifold  $[0, 1] \times \mathbb{S}^1$  to the 3-manifold  $[0, 1] \times \mathbb{T}^2$ . By applying a small perturbation to this composite map, it can be put into general position for almost all  $t \in [0, 1]$ . The remaining ‘non-generic diagrams’ in  $\{t\} \times \mathbb{T}^2$  for finitely many  $t$ ’s will be dealt with using the five  $R$ -moves.

Note that some cases of non-regularity of a projection in  $\{t\} \times \mathbb{T}^2$  are due to the singularities of the map  $[0, 1] \times \mathbb{S}^1 \longrightarrow [0, 1] \times \mathbb{T}^2$ . To understand those singularities, a key local result we will use in our proof is the following theorem by Whitney.

**Theorem 3.13** (Whitney, [41]). *Let  $W$  be a smooth 2-manifold and  $Y$  a smooth 3-manifold. Any smooth map  $g_0 : W \longrightarrow Y$  can be approximated arbitrarily closely (in the  $C^2$  topology) by a smooth map  $g : W \longrightarrow Y$  with the following property. Around each point  $p \in W$ , there are local coordinates  $(x, y)$  so that  $p$  corresponds to  $(0, 0)$ , and there are local coordinates  $(u, v, z)$  around  $g(p) \in Y$ , so that  $(0, 0, 0)$  corresponds*

to  $g(p)$ , with respect to which the function  $g$  has the form  $(x, y) \mapsto (x, y, 0)$  or  $(x, y) \mapsto (x^2, xy, y)$ .

Whitney's theorem can be understood as follows. Consider the Jacobian  $J_{g(p)} : T_p W \rightarrow T_{g(p)} Y$  of the map  $g$  at  $p \in W$ . On the one hand, it is clear that points of the first kind are those for which the Jacobian is injective, and so, at those points  $g$  is an immersion. On the other hand, points of the second kind are the singular points of  $g$ , where the Jacobian has a 1-dimensional kernel. Note that for a generic choice of  $g$ , the rank of  $J_{g(p)}$  is non-zero for all  $p \in W$ . Thus, Whitney's theorem gives a canonical form for the neighbourhood of the singular points of  $g$ , depicted in Figure 13. Such a singularity is called a *Whitney umbrella*. A proof of Theorem 3.13 is given in [36].

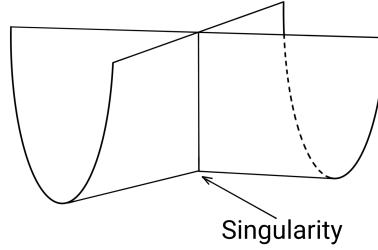


Figure 13: The Whitney umbrella. It is the image of the map  $(x, y) \mapsto (x^2, xy, y)$ .

**Proof Proof of Theorem 3.12.** Suppose that  $D$  is the diagram of the smoothly embedded link with one component  $\Gamma$ . Assuming that  $\Gamma'$  is ambient isotopic to  $\Gamma$ , the same projection map yielding  $D$  from  $\Gamma$  yields a diagram  $D'$  from  $\Gamma'$ . Regard the isotopy  $f : [0, 1] \times \mathbb{S}^1 \rightarrow [0, 1] \times \mathbb{T}^3$  between the links as a smoothly embedded surface-with-boundary with the following properties:

- (1)  $\text{Im}(f) \cap (\{0\} \times \mathbb{T}^3) = \{0\} \times \Gamma$ ,
- (2)  $\text{Im}(f) \cap (\{1\} \times \mathbb{T}^3) = \{1\} \times \Gamma'$  and
- (3) the intersection  $f([0, 1] \times \mathbb{S}^1) \cap (\{t\} \times \mathbb{T}^3)$  is transverse for all  $t \in [0, 1]$ .

Consider the projection map  $pr_1 : [0, 1] \times \mathbb{T}^3 \rightarrow [0, 1]$ . Property (3) is in fact a reformulation of the fact that  $pr_1 \circ f : [0, 1] \times \mathbb{S}^1 \rightarrow [0, 1]$  has no critical points. Indeed, if  $y \in f([0, 1] \times \mathbb{S}^1) \cap (\{t\} \times \mathbb{T}^3)$ , as  $T_y \{t\} \times \mathbb{T}^3$  has dimension 3, Property (3) is true if and only if  $T_y f([0, 1] \times \mathbb{S}^1)$  is of dimension greater or equal to 1 and is not a subspace of  $T_y \{t\} \times \mathbb{T}^3$ . This is equivalent to  $T_y f([0, 1] \times \mathbb{S}^1) \cap T_y [0, 1] \neq \{0\}$ . This occurs if and only if  $T_y pr_1 \circ f([0, 1] \times \mathbb{S}^1) \neq \{0\}$ , which is the characterisation of

$pr_1 \circ f$  having no critical points, meaning that  $pr_1 \circ f$  is a submersion. Now recall that being a submersion is an open property [19] which means that a small perturbation of  $f$  does not have a critical point.

Furthermore, pictorially, consider  $t \in [0, 1]$  of  $[0, 1] \times \mathbb{T}^3$  as the ‘variation of time’. By doing so,  $\{t\} \times \mathbb{T}^3$  has a front face indexed by  $t$  which we call *t-front face*  $\{t\} \times \mathbb{S}_1^1 \times \mathbb{S}_2^1 \times \{0 + \varepsilon\}$ , a back face indexed by  $t$  which we call *t-back face*  $\{t\} \times \mathbb{S}_1^1 \times \mathbb{S}_2^1 \times \{1 - \varepsilon\}$ ,  $\varepsilon > 0$ , and a *t-N-face*  $\{t\} \times \mathbb{S}_1^1 \times \mathbb{S}_2^1 \times \{N\}$  extending Definition 3.1 for all  $t \in [0, 1]$ .

We now extend the projection map  $\pi : \mathbb{T}^3 \longrightarrow \mathbb{T}^2$  defining the diagram to the map  $P = Id \times \pi : [0, 1] \times \mathbb{T}^3 \longrightarrow [0, 1] \times \mathbb{T}^2$ , and compose the embedding  $f$  of the annulus  $[0, 1] \times \mathbb{S}^1$  with  $P$  to get a map  $\phi = P \circ f : [0, 1] \times \mathbb{S}^1 \longrightarrow [0, 1] \times \mathbb{T}^2$ . Theorem 3.12 is proved by applying Theorem 3.13 to this map  $\phi$ , as follows.

Since  $P$  is a submersion,  $\phi$  can be put into general position by slightly perturbing the map  $f$ , so that it remains an isotopy between  $\Gamma$  and  $\Gamma'$ . This is possible thanks to the three properties of  $f$  listed above as explained in [38]. Theorem 3.13 shows that there are finitely many points  $\mathcal{W} \subset [0, 1] \times \mathbb{S}^1$  with a Whitney umbrella singularity, away from which the map  $\phi$  is an immersion. By a further general position argument, we can assume that  $\phi$  has only finitely many triple points (ie points in  $[0, 1] \times \mathbb{T}^2$  with three preimages), and a union of 1-dimensional submanifolds  $\mathcal{D} \subset [0, 1] \times \mathbb{T}^2$  of double points. The closure of the set of double points includes the set of triple points and the set of Whitney umbrella singularities. Its boundary also includes the double points  $\mathcal{D} \cap (\{0\} \times \mathbb{T}^2)$ ,  $\mathcal{D} \cap (\{1\} \times \mathbb{T}^2)$  of the two original diagrams  $D$  and  $D'$ .

Regard the intersections  $\phi([0, 1] \times \mathbb{S}^1) \cap (\{t\} \times \mathbb{T}^2)$  as a 1-parameter family of diagrams. Again, by general position arguments, there are finitely many special  $t \in [0, 1]$  where these diagrams are not generic, and where exactly one of the following occurs:

- (1)  $\phi^{-1}(\{t\} \times \mathbb{T}^2)$  contains a Whitney umbrella singularity,
- (2)  $\phi([0, 1] \times \mathbb{S}^1) \cap (\{t\} \times \mathbb{T}^2)$  contains a triple point,
- (3)  $\{t\} \times \mathbb{T}^2$  is tangent to  $\mathcal{D}$ ,
- (4)  $\phi([0, 1] \times \mathbb{S}^1) \cap (\{t\} \times \mathbb{T}^2)$  contains a double point for which the embedding in  $\{t\} \times \mathbb{T}^3$  of one of the two elements of its preimage is lying in the *t-N-face*,

- (5)  $\phi([0, 1] \times \mathbb{S}^1) \cap (\{t\} \times \mathbb{T}^2)$  contains a point such that the  $t$ - $N$ -face is tangent to the embedding of the preimage of that point in  $\{t\} \times \mathbb{T}^3$ .

Consider  $0 \leq t_1 < t_2 \leq 1$ , and suppose that there are no special values of  $t \in [t_1, t_2]$ . In this case, as  $\phi$  is an immersion and thus locally an embedding, the projections at  $t_1$  and  $t_2$  are connected by planar isotopies.

Assume next that the interval  $[t_1, t_2]$  contains a single special value. Suppose that the special value corresponds to a Whitney umbrella singularity as in (1). Furthermore, assume that at that value  $t$ ,  $\{t\} \times \mathbb{T}^2$  is transverse to the 1-dimensional image of the Jacobian. Then the diagrams  $\phi([0, 1] \times \mathbb{S}^1) \cap \{t_1\} \times \mathbb{T}^2$  and  $\phi([0, 1] \times \mathbb{S}^1) \cap \{t_2\} \times \mathbb{T}^2$  differ by a single  $R_1$  move as seen in Figure 14a. Indeed the Whitney umbrella singularity occurs when a crossing is being taken out or added to the family of diagrams.

Next, as  $\{t\} \times \mathbb{T}^2$  passes through a point of tangency with  $\mathcal{D}$  as given by (2), the projection undergoes an  $R_2$  move as shown in Figure 14b.  $\{t\} \times \mathbb{T}^2$  is tangent to  $\mathcal{D}$  exactly when two crossings are deleted or added to the family of diagrams.

In the case (3), a triple point is locally modelled on three intersecting planes as in Figure 14c. The diagrams  $\phi([0, 1] \times \mathbb{S}^1) \cap \{t_1\} \times \mathbb{T}^2$  and  $\phi([0, 1] \times \mathbb{S}^1) \cap \{t_2\} \times \mathbb{T}^2$  differ by an  $R_3$  move. A triple point occurs when one strand passes through the crossing of other two strands in the family of diagrams.

Assume now that the special value corresponds to the case (4). The projections in  $\{t_1\} \times \mathbb{T}^2$  and  $\{t_2\} \times \mathbb{T}^2$  differ by an  $R_4$  move. Indeed, such a double point appears when a strand passes between the front part and back part of another strand as shown in Figure 15a.

Finally, as the  $t$ - $N$ -face passes through a point of tangency with the component of the link, as given in (5), the projection undergoes an  $R_5$  move. This happens exactly when a strand goes through the  $N$ -face as seen in Figure 15b.  $\square$

**Remark 3.14** Strictly speaking, in the proof of Theorem 3.12 there still are some non-regular projections in the 1-parameter family of diagrams. For example, when there is a tangent intersection or a double point on the borders of the square  $\mathbb{T}^2$ . However, those do not need any special moves as they arise only because of our choice of

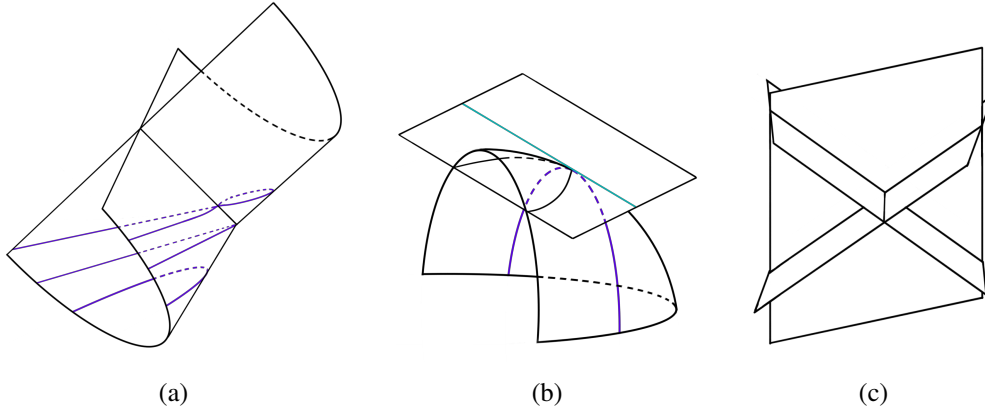


Figure 14: Non-generic occurrences: (A) The Whitney umbrella and the  $R_1$  move. We can assume that the singularity is transverse to the projection. (B) The double point set of the projection. When crossing the double point set with a plane (locally), we get crossings in the projection. When  $\{t\} \times \mathbb{T}^2$  is tangent to the double point set, we get an  $R_2$  move. (C) A triple point locally modelled by three intersecting planes. This corresponds the  $R_3$  move.

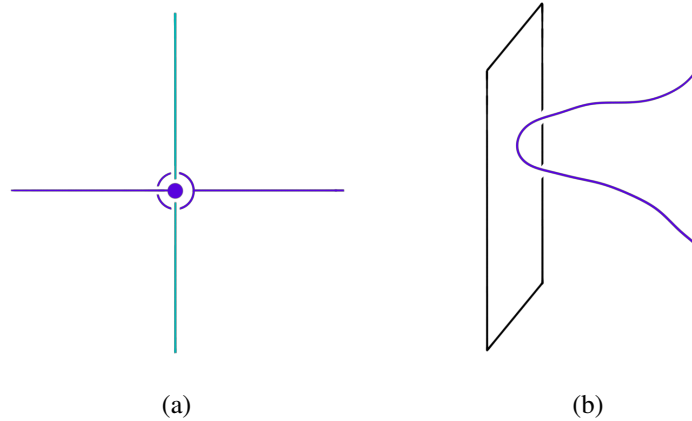


Figure 15: Non-generic occurrences: (A) A strand goes between the front part and back part of another that intersects the  $t$ - $N$ -face. This requires the  $R_4$  move. (B) The  $t$ - $N$ -face is tangent to a strand. This corresponds to the  $R_5$  move.

representation of the torus. One can glue the square of the diagram into an actual torus and forget the borders of the square.

Theorem 3.12 states that ambient isotopies in  $\mathbb{T}^3$  translate to  $R$ -moves and planar isotopies in a diagram. However, some other 3 dimensional transformations, such as torus twists for example, require more than one diagram as it is very difficult to translate them into simple transformations with a single one. This motivates the following definition.

**Definition 3.15** A *tridiagram* of a 3-periodic tangle, here seen as an exact embedding and not an equivalence class, is a set of three non-equivalent diagrams drawn out of a three regular projections of a unit cell along three non-coplanar axes.

**Lemma 3.16** A *tridiagram* is well defined. Furthermore, from any diagram  $A$ , one can associate a *tridiagram*  $\{A, B, C\}$ .

**Proof** All  $R$ -moves (along with planar isotopies) have been created to mimic ambient isotopies. Therefore, all equivalent diagrams represent equivalent TP tangles. Conversely, Theorem 3.12 states that isotopic unit cells give equivalent diagrams projected along the same axis.

For a TP tangle  $K$  and an associated unit cell  $U$ , one can make three projections along three non-coplanar axes, say  $\{A, B, C\}$ . However those projections are not necessarily regular. If one projection is not regular, say  $A$ , one can slightly deform  $U$  to get an isotopic unit cell  $U'$  to obtain a regular projection  $A'$ . The resulting set  $\{A', B, C\}$  is a tridiagram that represents accurately the isotopic unit cells  $U$  and  $U'$  as explained by the previous remark.

The second part of the lemma is immediate. One can embed  $A$  as a link in  $\mathbb{T}^3$  and draw out two other diagrams from that embedding, and thus, can obtain a tridiagram  $\{A, B, C\}$ .  $\square$

**Remark 3.17** The associated tridiagram to a diagram  $A$  need not be unique, as there are infinitely many ways of embedding  $A$ .

**Definition 3.18 (Equivalence of tridiagrams)**

Two tridiagrams  $\{D_i\}_{i=1,2,3}$  and  $\{D'_i\}_{i=1,2,3}$  are *equivalent* if there is a finite sequence of tridiagrams  $(\{D_{i,k}\}_{i=1,2,3})_{k=0,\dots,n}$ , for which we have

$$D_{i,0} = D_i, \quad D_{i,n} = D'_i, \quad i = 1, 2, 3$$

and

$$\forall k = 1, \dots, n, \exists i, j = 1, 2, 3 : D_{i,k-1} \sim_D D_{j,k}.$$

### 3.3 Generalised Reidemeister theorem

We are now in a position to give a generalised Reidemeister theorem for TP tangles.

**Theorem 3.19 (Generalised Reidemeister theorem)**

*Two 3-periodic tangles  $K$  and  $K'$  are equivalent if and only if any two of their respective tridiagrams  $\{D_i\}_{i=1,2,3}$  and  $\{D'_i\}_{i=1,2,3}$  are equivalent.*

**Proof** One implication is quite immediate. If we have two equivalent tridiagrams, there exists a finite sequence of tridiagrams satisfying the conditions of equivalence given in Definition 3.18. But the  $R$ -moves and 2-torus isotopies, 2-torus twists,  $M^2$ -equivalence and  $V$ -equivalence respectively translate the 3-torus isotopies, 3-torus twists,  $M^3$ -equivalence and change of face onto which the projection is made. Therefore, the associated embeddings  $K$  and  $K'$  are also equivalent.

Now for the converse, consider  $\Gamma_{k-1}$  and  $\Gamma_k$  two links in  $\mathbb{T}^3$  as in Definition 2.17. If they are connected by ambient isotopies, then Theorem 3.12 and Lemma 3.16 settle the problem. Otherwise, if they are connected by torus twists, we recall that the following shear matrices generate  $SL(3, \mathbb{Z})$ .

$$M_1 = \begin{bmatrix} 1 & 1 & 0 \\ 0 & 1 & 0 \\ 0 & 0 & 1 \end{bmatrix}, \quad M_2 = \begin{bmatrix} 1 & 0 & 0 \\ 1 & 1 & 0 \\ 0 & 0 & 1 \end{bmatrix}, \quad M_3 = \begin{bmatrix} 1 & 0 & 1 \\ 0 & 1 & 0 \\ 0 & 0 & 1 \end{bmatrix},$$

$$M_4 = \begin{bmatrix} 1 & 0 & 0 \\ 0 & 1 & 0 \\ 1 & 0 & 1 \end{bmatrix}, \quad M_5 = \begin{bmatrix} 1 & 0 & 0 \\ 0 & 1 & 1 \\ 0 & 0 & 1 \end{bmatrix}, \quad M_6 = \begin{bmatrix} 1 & 0 & 0 \\ 0 & 1 & 0 \\ 0 & 1 & 1 \end{bmatrix}.$$

Clearly each one of these matrices can be seen as a planar transformation, and thus can be translated to a 2-torus twist. For illustration, suppose that  $\Gamma_{k-1}$  and  $\Gamma_k$  are connected by the sequence of 3-torus twists associated to  $M_4 M_1$ . We can assume that their respective tridiagrams are  $\{D_z, D_x, D_y\}$  and  $\{D'_z, D'_x, D'_y\}$  with  $x, y, z$  indicating the axis of projection.

The action of  $M_1$  (or rather  $\phi_{M_1}$  as in Subsection 2.2) on  $\Gamma_{k-1}$  can be seen as a 2-torus twist of  $\begin{bmatrix} 1 & 1 \\ 0 & 1 \end{bmatrix}$  on  $D_z$ . We call the resulting diagram  $D_{2,z}$ . From the latter, thanks to Lemma 3.16, one can get a tridiagram  $\{D_{2,z}, D_{2,x}, D_{2,y}\}$ .

Similarly, the action of  $M_4$  on  $\phi_{M_1}(\Gamma_{k-1})$  can be translated to a 2-torus twist of  $\begin{bmatrix} 1 & 0 \\ 1 & 1 \end{bmatrix}$  on  $D_{2,y}$ . The resulting diagram is  $D'_y$ . Thus we get a finite sequence of tridiagrams satisfying the equivalence for tridiagrams.

Now if  $\Gamma_{k-1}$  and  $\Gamma_k$  satisfy the conditions of  $M^3$ -equivalence given in Definition 2.14, the process is similar to the previous one for torus twists but with the  $M^2$ -equivalence, by cutting or gluing copies of each diagram of the tridiagrams.

Lastly, for a given unit cell, there are six faces. To obtain a tridiagram, one has three sets of opposite faces. The choice of projection along which opposite face is described by the  $V$ -equivalence.  $\square$

## 4 Invariants for 3-periodic tangles

The notions of diagrams and tridiagrams described in Section 3 enable the description of some simple invariants for 3-periodic tangles, including the *minimum number of components*, the *crossing number* and the *unknotting number*. We also discuss here some challenges related to the *linking number* for 3-periodic tangles.

### 4.1 Minimum number of components

The first invariant to consider is the minimum number of components of a TP tangle. In the case of usual links in 3-space, the number of components is readily defined and is an invariant [32]. The definition has been generalised to DP tangles in [18]. For TP tangles, defining the minimum number of components of a TP tangle relates to finding its most refined lattice  $\mathcal{L}^*$ .

**Definition 4.1** The *minimum number of components* of a TP tangle is defined as the number of components of any unit cell or diagram associated to the lattice  $\mathcal{L}^*$ .



**Proposition 4.2** *The minimum number of components is well defined and is an invariant of 3-periodic tangles.*

**Proof** Firstly, within a unit cell, there is no ambient isotopy that would change the number of components of a link in the 3-torus by definition. Secondly, a torus twist winds and unwinds curves around the ‘hole’ of the torus as in Figure 4, which does not change the number of components. Those two previous points are also true for diagrams, and as a unit cell contains a fixed number of curves, any projection along any axis has the same number of curves. It is clear then that only a change of lattice would possibly change the number of components, and this justifies the choice of the most refined lattice  $\mathcal{L}^*$ .  $\square$

## 4.2 Crossing number

We now consider the crossing number, which is previously defined as the minimum number of crossings over all diagrams of a knot [33]. It has also been defined for DP tangles in [18] and for specific cases of DP weaves [30]. Moreover, it has also been shown to be related to the volume of *weaving knots*, that are alternating link diagrams of torus links representing unit cells of alternating and biaxial DP weaves, and thus to the volume of these particular DP tangles [5]. The crossing number is the main complexity ordering of finite knots and links.

**Definition 4.3** To a tridiagram, one can associate an unordered triplet of numbers of crossings  $(a, b, c)$ . It is referred to as a *triplet of crossings*. We define the *crossing number* as the minimum of  $a^2 + b^2 + c^2$  among all triplets of crossings of a 3-periodic tangle. A triplet realising the crossing number is called a *minimum crossing number triplet*.

We note that the circle symbol representing the curve passing through the front and back faces depicted in Figure 8 is not considered a crossing.

We now motivate our definition of crossing number. Firstly, considering our characterisation of 3-periodic tangles via tridiagrams, three crossing numbers are necessary to describe the entanglement. Indeed, some 3-periodic tangles, such as the ones shown in Figure 16, have particular diagrams with no crossings, but cannot have a tridiagram with a  $(0, 0, 0)$  crossing triplet where all three diagrams have no crossing simultaneously.

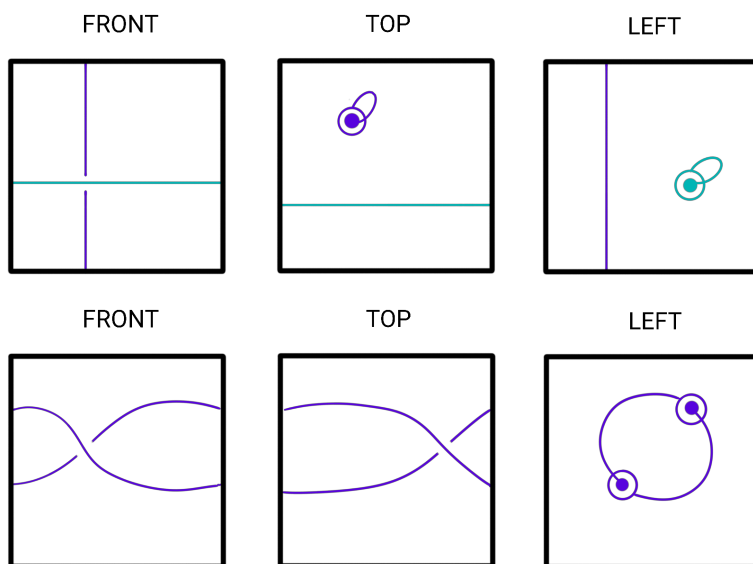


Figure 16: Examples of 3-periodic tangles possessing one diagram having no crossings but with no tridiagrams with no crossings. On the top, a tridiagram of a bidirectional layer packing of straight lines. On the bottom, a tridiagram of a unidirectional packing of double helices.

Secondly, there can be many ways of minimising the number of crossings of tridiagrams. However, we choose the sum of squares to bias the triplet towards a type  $(a, a, a)$  where possible, favouring a symmetric configuration.

In general, symmetric embeddings of the structure tend to decrease the number of crossings. As an example consider the TP tangle of Figure 17, where we shear its associated lattice. Before shearing the lattice, the axes of the embedding are parallel to those of the unit cell, and the triplet of crossings is  $(0, 0, 1)$  as given by the tridiagram in Figure 17a. By shearing the lattice, we ‘break’ the symmetry of the TP tangle, and a crossing has been added as seen in Figure 17d. The resulting triplet of crossings is  $(0, 1, 1)$ .

### 4.3 Unknotting number

We will define here the unknotting number of 3-periodic tangles using the diagrams. The unknotting number for finite knots has been defined as the least number of crossings to be changed among all diagrams of a knot to transform it into the unknot [33]. By changing a crossing, we mean inverting the over-strand and under-strand defining the crossing. This definition has been extended to DP tangles in [18].

We recall that the operation of changing a crossing of a knot is called an *unknotting operation*. We extend naturally this operation to the diagrams of 3-periodic tangles. It is clear that an unknotting operation reduces or preserves the number of crossings of a diagram.

Consider a diagram of a 3-periodic tangle  $K$ , of a tridiagram realising its crossing number. By applying one (and only one) unknotting operation to this diagram, one obtains another TP tangle  $K_1$  that possesses a crossing number less or equal to that of  $K$ .

**Definition 4.4** Given a sequence of TP tangles  $(K_k)_{k=0,\dots,n}$  with  $K_0 = K$ , related by unknotting operations as described above, we define the *unknotting number* of  $K$  as the smallest  $n$  over all possible sequences  $(K_k)_{k=0,\dots,n}$ , where for all  $k = 0, \dots, n-1$ , the crossing number of  $K_{k+1}$  is strictly less than that of  $K_k$ .

**Proposition 4.5** *The unknotting number is well defined and is an invariant.*

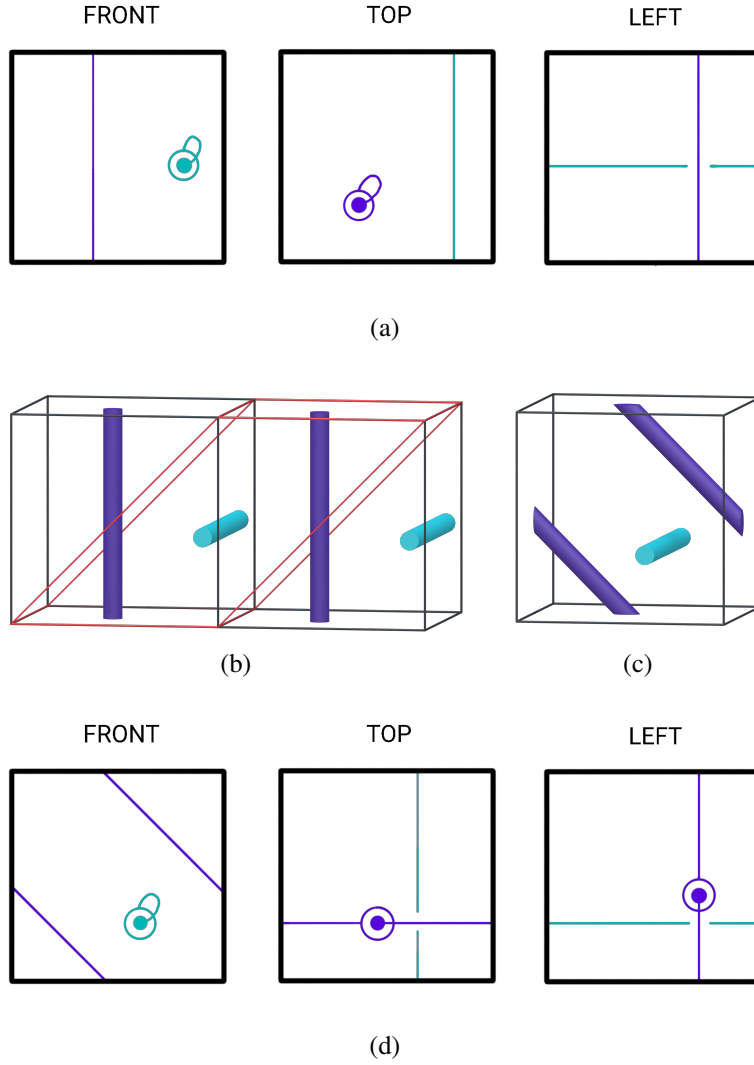


Figure 17: (A) A tridiagram of a bidirectional layer packing of straight lines, which has triplet of crossings  $(0, 0, 1)$ . (B) A shearing of the lattice which would correspond to a torus twist in the unit cell. (C) The resulting unit cell after torus twist. (D) A tridiagram of the sheared unit cell, which now has triplet of crossings  $(0, 1, 1)$ .

**Proof** By definition the unknotting number is related to the crossing number. The crossing number is linked to the most refined lattice  $\mathcal{L}^*$ , as a diagram of this lattice has less number of crossings than a diagram of a greater volume. Therefore, as we consider only a diagram of the  $\mathcal{L}^*$  lattice of each  $K_k$ , the  $M^2$ -equivalence does not affect the unknotting number.

A torus twist generates crossings such as the ones in Figure 17d or in Figure 18c. An unknotting operation does not eliminate such crossings. As the definition of unknotting number requires that the crossing number of  $K_{k+1}$  is strictly less than that of  $K_k$ , an unknotting operation performed on such a crossing is not counted for the unknotting number.

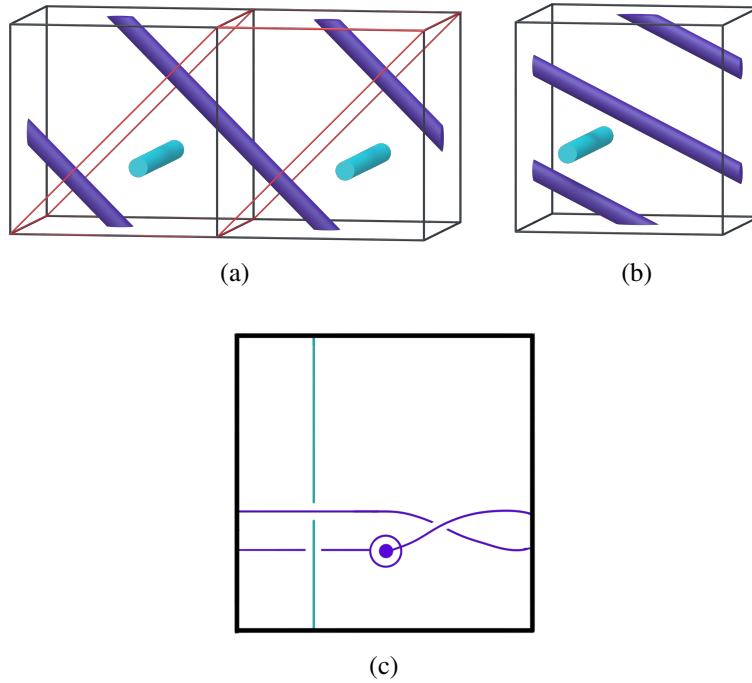


Figure 18: A torus twist applied on the unit cell of Figure 17c. (C) The top diagram of the unit cell of (B), displaying crossings that cannot be eliminated by an unknotting operation.

The unknotting operation is in fact a transformation realised in space where one swaps the positions of two curves. It is defined by the means of diagrams only because it is

in a diagram that a crossing is well defined and that the swapping of positions of two curves is actually equivalent to changing a crossing between the projections of those two curves. Therefore, working with a single diagram of a tridiagram realising the crossing number is enough. Furthermore, two  $V$ -equivalent diagrams have the exact same number of crossings. Performing an unknotting operation on one is equivalent to doing it on the other.

Therefore, an unknotting number is well defined and is an invariant.  $\square$

**Example 4.6** Figure 19 shows a 3-periodic tangle to which we change a crossing to get the structure unknotted. Thus the unknotting number is 1.

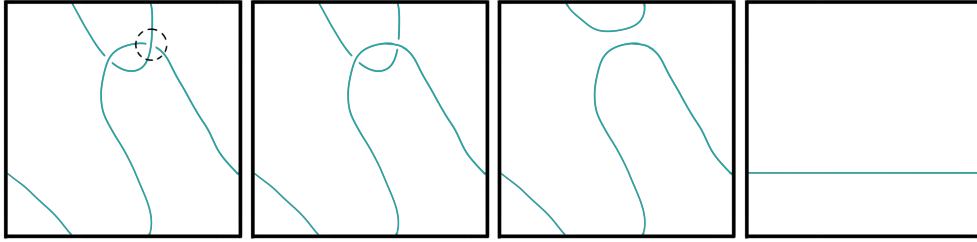


Figure 19: Unknotting a 3-periodic tangle to a packing of straight lines.

**Example 4.7** Figure 20 gives an example of a 3-periodic tangle that has 0 as unknotting number. Indeed, an unknotting operation on this crossing does not reduce the crossing number.

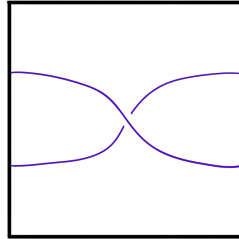


Figure 20: A diagram of a 3-periodic packing of double helices with its crossing that cannot be eliminated by an unknotting operation.

In fact, besides the packing of double helices and the 3-periodic packing of unknots, all 3-periodic tangles with only straight lines as components, ie the cylinder packings,

have 0 as an unknotting number. Indeed, consider a diagram of such a 3-periodic tangle and regard it as a usual 2-torus. Consider the curves that are not homotopic to a point. Unless their ‘axes’ are parallel, two such curves intersect and thus, there is a crossing between them. To see this, one can lift the curves in a doubly periodic way into a plane to get lines. Unless those lines have parallel axes, they intersect. Clearly, such an intersection cannot be deleted by an unknotting operation. And as such intersections are the only crossings of the diagram, the unknotting number is 0.

#### 4.4 Comments on the Linking number

For a usual oriented link in  $\mathbb{R}^3$  the linking number is half the sum of the signs of the crossings, displayed in Figure 21, between the link components [33].

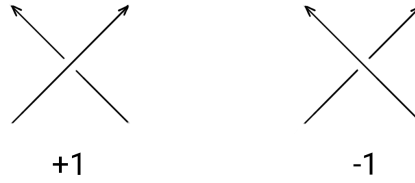


Figure 21: Signs of crossings between the components of an oriented link.

In fact, computing the signs of crossings simplifies the more general definition given by Gauss using a double integral, which makes sense even for open curves [3]. The *Gauss linking number* [15] of two disjoint oriented curves  $l_1$  and  $l_2$ , whose arc-length parametrisations are  $\gamma_1(t)$ ,  $\gamma_2(s)$  respectively, is defined as a double integral over  $l_1$  and  $l_2$ ,

$$L(l_1, l_2) = \frac{1}{4\pi} \int_0^1 \int_0^1 \frac{\det(\gamma'_1(t), \gamma'_2(s), \gamma_1(t) - \gamma_2(s))}{\|\gamma_1(t) - \gamma_2(s)\|^3} dt ds,$$

where  $\gamma'_i$  is the vector derivative of  $\gamma_i$ .

Using this double integral, the linking number has been extended as a measure (and not an invariant) to periodic systems in [35].

Considering the new diagrammatic description for TP tangles given in this paper, one wishes to refine the definition of linking number for periodic systems by computing the

signs of crossings in a diagram. However, this cannot always be done.

In Figure 22a, we give an example where we can change the nature of the crossing between the components of the link by using only  $R$ -moves and planar isotopies. Defining the linking number in terms of signs of crossings is therefore not possible. This is not a failure of the diagrams. On the contrary, the diagrams here capture well the property of a bidirectional layer packing of straight lines of having the same layer of horizontal lines in front of and behind a layer of vertical lines, as shown in Figure 22b and 22c.

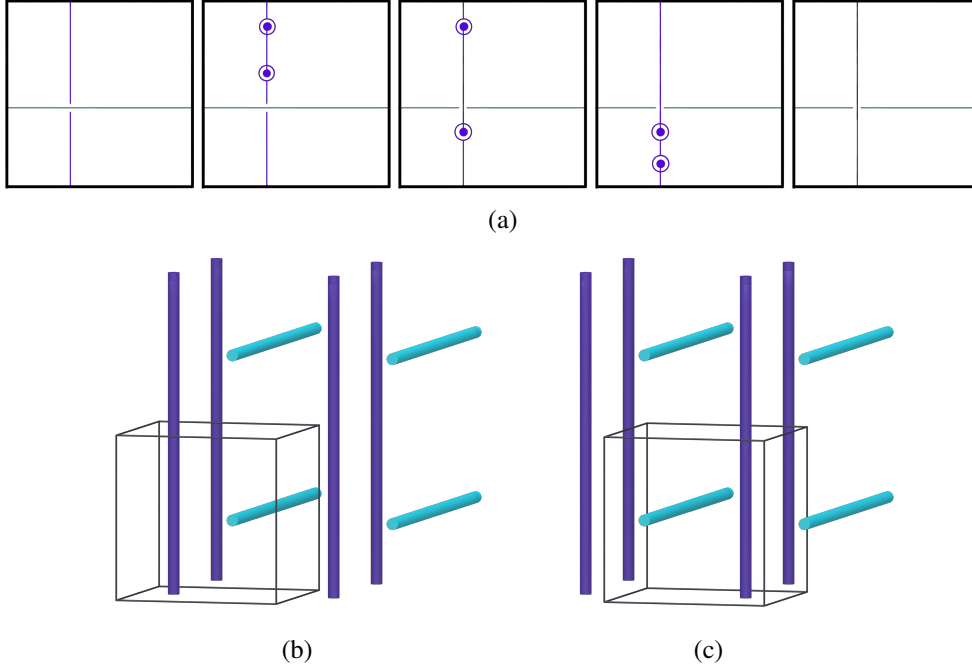


Figure 22: (A) Inverting the nature of the crossing between two components of the link in 3-torus using only  $R$ -moves and planar isotopies. (B) A bidirectional layer packing of lines with one unit cell shown in black. A projection from the right face of the unit cell gives the starting diagram above. (C) The same 3-periodic tangle with a different unit cell. A projection from the right face of this choice of unit cell gives the last diagram above.

**Remark 4.8** One may notice that actually the  $R_4$  move alone already inverts the nature of a crossing as in Figure 11a, and is the cause of inversion in Figure 22a.



## References

- [1] **C Adams**, *The knot book: An elementary introduction to the mathematical theory of knots*, American Mathematical Society, Providence (2004)
- [2] **K Barkataki, E Panagiotou**, *The Jones polynomial in systems with Periodic Boundary Conditions* (2023) Available at <https://arxiv.org/abs/2309.14572>
- [3] **M Bright, O Anosova, V Kurlin**, *A Formula for the Linking Number in Terms of Isometry Invariants of Straight Line Segments*, Computational Mathematics and Mathematical Physics 62 (2022) 1217–1233
- [4] **G Burde, H Zieschang, M Heusener**, *Chapter 1: Knots and isotopies*, from “Knots”, De Gruyter, Berlin, Boston (2013) 1–15
- [5] **A Champanerkar, I Kofman, J Purcell**, *Volume bounds for weaving knots*, Algebraic & Geometric Topology 16 (2016) 3301–3323
- [6] **I Diamantis, S Lambropoulou, S Mahmoudi**, *Equivalence of Doubly Periodic Tangles* (2023) Available at <https://arxiv.org/abs/2310.00822>
- [7] **M Evans, S Hyde**, *From three-dimensional weavings to swollen corneocytes*, Journal of The Royal Society Interface 8 (2011) 1274–1280
- [8] **M Evans, V Robins, S Hyde**, *Periodic entanglement II: weavings from hyperbolic line patterns*, Acta Crystallographica Section A 69 (2013) 262–275
- [9] **M Evans, R Roth**, *Shaping the Skin: The Interplay of Mesoscale Geometry and Corneocyte Swelling*, Phys. Rev. Lett. 112 (2014) 038102
- [10] **B Farb, D Margalit**, *Chapter 1: Curves, Surfaces, and Hyperbolic Geometry*, from “A Primer on Mapping Class Groups (PMS-49)”, Princeton University Press, Princeton (2012) 17–43
- [11] **B Farb, D Margalit**, *Chapter 2: Mapping Class Group Basics*, from “A Primer on Mapping Class Groups (PMS-49)”, Princeton University Press, Princeton (2012) 44–63
- [12] **B Farb, D Margalit**, *Chapter 3: Dehn Twists*, from “A Primer on Mapping Class Groups (PMS-49)”, Princeton University Press, Princeton (2012) 64–88
- [13] **M Fukuda, M Kotani, S Mahmoudi**, *Classification of doubly periodic untwisted  $(p,q)$ -weaves by their crossing number and matrices*, Journal of Knot Theory and Its Ramifications 32 (2023) 2350032
- [14] **M Fukuda, M Kotani, S Mahmoudi**, *Construction of weaving and polycatenane motifs from periodic tilings of the plane* (2023) Available at <https://arxiv.org/abs/2206.12168>
- [15] **C F Gauss**, *Integral formula for linking number*, Zur mathematischen theorie der electrodynamische wirkungen, Collected Works 5 (1833) 605
- [16] **S Grishanov, V Meshkov, A Omelchenko**, *Kauffman-type polynomial invariants for doubly periodic structures*, Journal of Knot Theory and Its Ramifications 16 (2007) 779–788

- [17] **S Grishanov, V Meshkov, A Omelchenko**, *A Topological Study of Textile Structures. Part I: An Introduction to Topological Methods*, Textile Research Journal 79 (2009) 702–713
- [18] **S Grishanov, V Meshkov, A Omelchenko**, *A Topological Study of Textile Structures. Part II: Topological Invariants in Application to Textile Structures*, Textile Research Journal 79 (2009) 822–836
- [19] **V Guillemin, A Pollack**, *Chapter 1: Manifolds and smooth maps*, from “Differential Topology”, American Mathematical Society, Providence (1974) 1–56
- [20] **V Guillemin, A Pollack**, *Chapter 2: Transversality and intersection*, from “Differential Topology”, American Mathematical Society, Providence (1974) 57–93
- [21] **P Guillot**, *Partie I. 5: La classification des revêtements*, from “Leçons sur l’homologie et le groupe fondamental”, Société Mathématique de France, France (2022) 77–89
- [22] **M Hirsch**, *Chapter 2: Function Spaces*, from “Differential Topology”, Springer New York, New York, NY (1976) 34–66
- [23] **M Hirsch**, *Chapter 3: Transversality*, from “Differential Topology”, Springer New York, New York, NY (1976) 67–84
- [24] **C O Y Hui, J S Purcell**, *On the geometry of rod packings in the 3-torus* (2023) Available at <https://arxiv.org/abs/2212.04662>
- [25] **S Lambropoulou, C P Rourke**, *Markov’s theorem in 3-manifolds*, Topology and its Applications 78 (1997) 95–122 Braid Groups and Related Topics
- [26] **J Lee**, *Chapter 3: New Spaces from Old*, from “Introduction to Topological Manifolds”, Springer New York, New York, NY (2011) 49–84
- [27] **R Lickorish**, *An Introduction to Knot Theory*, Springer, New York, NY (1997)
- [28] **A Likhtman, M Ponmurugan**, *Microscopic Definition of Polymer Entanglements*, Macromolecules 47 (2014) 1470–1481
- [29] **B Lu, S Vecchioni, Y Ohayon, R Sha, K Woloszyn, B Yang, C Mao, N Seeman**, *3D Hexagonal Arrangement of DNA Tensegrity Triangles*, ACS Nano 15 (2021) 16788–16793 PMID: 34609128
- [30] **S Mahmoudi**, *On the classification of periodic weaves and universal cover of links in thickened surfaces* (2023) Available at <https://arxiv.org/abs/2009.13896>
- [31] **H Morton, S Grishanov**, *Doubly periodic textile structures*, Journal of Knot Theory and Its Ramifications 18 (2009) 1597–1622
- [32] **K Murasugi**, *Chapter 1: Fundamental Concepts of Knot Theory*, from “Knot Theory and Its Applications”, Birkhäuser Boston, Boston, MA (1996) 5–24
- [33] **K Murasugi**, *Chapter 4: Classical Knot Invariants*, from “Knot Theory and Its Applications”, Birkhäuser Boston, Boston, MA (1996) 47–74

- [34] **M O’Keeffe, J Plévert, Y Teshima, Y Watanabe, T Ogama**, *The invariant cubic rod (cylinder) packings: symmetries and coordinates*, Acta Crystallographica Section A 57 (2001) 110–111
- [35] **E Panagiotou**, *The linking number in systems with Periodic Boundary Conditions*, Journal of Computational Physics 300 (2015) 533–573
- [36] **A S Peter Ozsváth, Z Szabó**, *Appendix B: Basic theorems in knot theory*, from “Grid Homology for Knots and Links”, American Mathematical Society, Providence (2015) 367–397
- [37] **D Rolfsen**, *Chapter 9: 3-Manifolds on surgery on links*, from “Knots and Links”, American Mathematical Society, Providence (1976) 233–283
- [38] **D Roseman**, *Elementary moves for higher dimensional knots*, Fundamenta Mathematicae 184 (2004) 291–310
- [39] **N Seeman**, *Nucleic acid junctions and lattices*, Journal of Theoretical Biology 99 (1982) 237–247
- [40] **R Thom**, *Un lemme sur les applications différentiables*, Bol. Soc. Mat. Mex., II. Ser. 1 (1956) 59–71
- [41] **H Whitney**, *The General Type of Singularity of a Set of  $2n - 1$  Smooth Functions of  $n$  Variables*, from “Hassler Whitney Collected Papers” (J Eells, D Toledo, editors), Birkhäuser Boston, Boston, MA (1992) 311–322

University of Potsdam, Institute for Mathematics, Karl-Liebknecht-Str. 24-25, 14476 Potsdam-Golm, Germany

University of Potsdam, Institute for Mathematics, Karl-Liebknecht-Str. 24-25, 14476 Potsdam-Golm, Germany

Advanced Institute for Materials Research (WPI-AIMR), Tohoku University, 2-1-1 Katahira, Aoba-Ku, Sendai, 980-8577, Japan

[evans@uni-potsdam.de](mailto:evans@uni-potsdam.de)